ResearchOnline@JCU

JAMES COOK UNIVERSITY AUSTRALIA

This is the author-created version of the following work:

Mamtani, Kapil, Farid, Mohammed M., and Shahbaz, Kaveh (2023) ***Application of Quaternary Ammonium-Based Deep Eutectic Solvents as Catalysts for the Glycerolysis of Free Fatty Acids.*** **Energy & Fuels, 37 pp. 7848-7855.**

Access to this file is available from:

https://researchonline.jcu.edu.au/86781/

© 2023 American Chemical Society

Please refer to the original source for the final version of this work:

https://doi.org/10.1021/acs.energyfuels.3c00666

Application of quaternary ammonium-based deep eutectic solvents as catalysts for the glycerolysis of free fatty acids

Kapil Mamtani[1], Mohammed M. Farid[1], Kaveh Shahbaz[1, 2*]

[1]Department of Chemical and Materials Engineering, The University of Auckland, Auckland 1010, New Zealand

[2]Circular Innovations (CIRCUIT) Research Centre, The University of Auckland, Auckland 1010, New Zealand

Abstract

Non-edible waste sourced lipids such as fatty acid distillates, brown grease, and animal tallow, among many others, are excellent alternatives for expanding the feedstock inventory for biodiesel synthesis. A quaternary ammonium-based Deep Eutectic Solvents (DESs) was used as a catalyst in the glycerolysis of free fatty acids in this study (FFAs). Reaction optimization was carried out with oleic acid as the model molecule, followed by an in-depth examination of the reaction mechanism. Optimum conditions: 130 °C, 10 wt. % catalyst dosage with 10 minutes of reaction time gave an equilibrium conversion of 94%. Catalyst was found to remain in the glycerol phase allowing its reuse. Palm fatty acid distillate, brown grease, and crude glycerol were utilized for testing the novel DES at optimum conditions. FFAs conversion were found to be 94% for both palm fatty acid distillate and brown grease. In the case of crude glycerol, FFAs conversion decreased proportionally to impurity level. Water was responsible for restricting equilibrium conversion and decreasing catalyst recyclability, necessitating further research into effective removal during the reaction. Aggressive nitrogen purging to remove water during the reaction pushed the reaction towards near completion in 60 minutes. The catalyst reusability study showed a drop in equilibrium conversion to 62.5% at the end of the 5th cycle, even when water was removed.

Keywords: Biodiesel; Deep eutectic solvents; Glycerolysis; Acid catalysis; Waste to energy.

*Corresponding author at: Chemical and Materials Engineering Department, The University of Auckland, Auckland 1010, New Zealand.
E-mail address: k.shahbaz@auckland.ac.nz (Kaveh Shahbaz)

1 Introduction

To keep up with the world's ever-increasing population, growing research scales, and improved lifestyle metrics, equally supporting energy supplies are required. Furthermore, as shown over the previous century, geopolitical landscapes and related energy reliance are extremely essential and dynamic, making energy independence imperative. Other sets of difficulties resulting from past centuries' industrial exploitations are anthropogenic climate change and the related risks to the Earth's environment, which necessitates a rapid shift to renewable energy sources. Bio-based energy sources have been of interest in much required transition to greener energy sources for many decades. Biodiesel, also known as fatty acid methyl esters (FAMEs), a petro-diesel alternative that is commercially synthesized from triglycerides derived mostly from vegetable oils such as canola, sunflower, and oil palm. [1-6]. The proven homogeneous transesterification method comes with a feedstock constraint due to the vulnerability of ester conversion during the reaction to the amount of free fatty acids (FFAs) present in the feed; as FFA% increases, FAMEs conversion decreases [7]. However, relying on pure vegetable oils as feed has been found unsustainable given their rising costs [8], food vs fuel disputes [9, 10], and growing deforestation for expanded farming activities [11]. Since feedstock prices make up around 75% of the cost of manufacturing, rising feedstock prices directly impact the price of biodiesel. These factors have slowed down biodiesel manufacturing worldwide, especially because sustainable feedstock supplies are scarce and seldom have comparable feed quality as that of pure vegetable lipids, thus requiring pretreatment [12-15]. Inedible sources of oils with varied FFAs levels have been proposed as a way to maintain biodiesel manufacturing and get around the problems aforementioned [16, 17]. Before application, feedstock’s containing FFAs must first undergo pretreatment since they impede the FAMEs conversion process. To convert FFAs to their respective alkyl esters, esterifying [18] with an alcohol is one of numerous chemical techniques mentioned in the literature. FFAs are esterified with an alcohol (usually methanol) with or without a catalyst, to form corresponding esters of FFAs, which can subsequently be sent for transesterification. Glycerolysis occurs when the alcohol moiety employed in esterification is glycerol (a prominent by-product of transesterification). The use of glycerol for pretreatment (glycerolysis) has the advantage of utilizing byproduct in-situ, which lowers losses [19]. Glycerol is substantially less soluble in organic solutions since it has three hydroxyl groups connected to it and is a hydrophilic molecule; per say, it is barely soluble to a 4-5 percent extent in ordinary hydrophobic lipids [20]. This low solubility impedes the reaction, subjected to high temperatures with or without the presence of a catalyst. Using Deep Eutectic Solvents (DESs) as a catalyst is one strategy for improving the glycerolysis reaction

within the constraints of green chemistry [21]. One of the review's [21] significant discoveries was that deep eutectic solvents—emerging green solvents—performed on par with the best-known catalysts (ionic liquids, metal derivatives, heteropolyacids, metal-organic frameworks, and others) in the glycerolysis. Mamtani et al. [22], confirmed similar findings, proving DESs as a worthy catalyst class in the esterification of FFAs. Compared to other catalysts, DESs provide benefits such as ease of preparation, low cost, and environmental friendly in manufacturing, operation, and disposal [23]. The successive significant findings published by Qin et al [24], Zhou et al [25], and Wang et al [26], involving development of bifunctional DESs for esterification of long chain esters, further support the decision of developing a DESs-based catalyst.

Reaction parameters have been carefully established in our past study efforts on non-catalytic glycerolysis of FFAs [27] and catalytic application of DESs in glycerolysis [28, 29]. With the set parameters, the DES catalyst based on allyltriphenyl phosphonium bromide and PTSAM (1:3 molar ratio) was shown to be best in catalysing the glycerolysis of oleic acid, achieving 95% equilibrium conversion in 30 minutes at 150 ℃ [28]. Thus, a feed of 6:1 M glycerol-to-fatty acid ratio and a 600 rpm agitation speed with an 80-120 mL/min N_2 purging rate were used. These variable settings and catalyst performance were recognised as the benchmark standard for furthering reaction improvements in the current study.

As a result, in this study, a new catalyst based on DESs was developed to improve the glycerolysis reaction. To determine the optimum conditions, the effect of altering catalyst concentration and temperature was investigated. Effect of water on equilibrium conversion was also examined. The important issue of catalyst reusability and its suitability for different feedstock were also investigated.

2 Experimental

2.1 Materials and apparatuses

2-Propanol (99.5%), glycerol (99.5%), n-hexane (≥99%), and potassium hydroxide (99%) were products of ECP Pt. Ltd. Analytical GC standards for monoolein (≥99%), diolein (≥99%) and oleic acid (≥99%) were purchased from Sigma-Aldrich (Australia). Technical olein (≥75%), p-toluene sulfonic acid monohydrate (PTSAM) (98.5%), phenolphthalein (≥95%), Tetra butyl ammonium hydrogensulphate (TBAHS) (97%) were purchased from Sigma-Aldrich (Australia). Brown grease was supplied by SabreEnergy, Australia. Crude glycerol grades were supplied by GreenFuels, New Zealand, and their composition is shown in Table 1. Palm fatty

acid distillates (PFAD) were supplied by Bakels Edible Oils, New Zealand. HYDRANAL-water standard (10.00 mg/g) for moisture determination was provided by Merck Pty Limited in glass ampoules. All the chemicals were used as supplied without any modification.

A batch reactor with auxiliary settings described in [28] was used with the exception of reactor volume being 250 mL in the present study. The following analytical instruments were used during this study: GC 2010 gas chromatograph (Shimadzu), Karl Fischer Moisture Analyzer (T5, Mettler Toledo), and UATR Two FT-IR instrument (PerkinElmer, used in the ATR mode for FT-IR).

Table 1. Composition of the studied crude glycerol grades.

Crude glycerol composition	Units	CG1	CG2
Glycerol	%mass	88.14	97.8
Ash	%mass	4.43	-
Water	%mass	3.72	2
Methanol	%mass	0.16	0.2
MONG, Matter Organic Non-glycerol	%mass	3.56	-

2.2 Method

In the present investigation, the batch reactor was provided with nitrogen purging using air flow meter maintained at 80-120 mL/minute rate. To establish reaction kinetics, oleic acid and pure glycerol were used as model reactants. Both reactants and catalyst were heated to the desired temperature separately and then mixed, marking the beginning of the reaction. The reaction mechanism was determined by sampling at the marked time intervals of 0, 5, 10, 15, 30, 45, 60, 90, 120, 150, and 180 min. Post reaction: The 5 mL samples were removed from the reactor and promptly quenched with ice to stop any reaction. The average of two independently repeated runs for each experimental condition was used to compute FFA conversion.

Following glycerolysis reaction and ice-quenching, the products consisted of an upper layer (i.e. mono-, di-, tri-glycerides and unreacted oleic acid) and a lower layer (i.e. excess glycerol and water). The upper layer was analysed for composition. The oleic acid [30] content was determined by the Lubrizol method for commercial fats and oils [31]. For the determination of glycerides content, the analysis was performed using a GC 2010 gas chromatograph equipped with split injection and flame ionisation detector (FID). Separation occurred using an Agilent

capillary DB-1HT column (15m, 0.25mm ID, 0.1 µm film thickness). Instrument grade helium was used as carrier gas at a constant flow of 30ml/min and the makeup gases consisted of hydrogen and dry air at constant flows of 40ml/min and 400ml/min, respectively. Sample volumes of 0.5 µL were injected at 290 ℃ with a split ratio of 20:1, while the FID detector was set to 380 ℃. The column oven temperature was programmed as follows: 50 °C held for 1 min; 100 °C at 50 °C/min; 220 °C at 80 °C/min; 290 °C at 30 °C/min; 330 °C at 50 °C/min and held 2 min; and 380 °C at 50 °C/min and held for 3 min. Linearity was established for standard solutions of oleic acid, monoolein, and diolein from 50 ppm to 1000 ppm and 1 mg/mL solutions of the product were taken from the upper layer using n-hexane as the solvent. The solution was then filtered through 0.22 µm PTFE filter and vialed GC analysis. Glyceride determination is reliant on interactions between internal column materials and particular glycerides. Analysis was done on duplicates. The greatest standard deviations for the doublets examined for all samples were less than 10%, and extremely good calibrations for GC-FID were obtained for monoolein (R^2, 0.999), diolein (R^2, 0.999), and oleic acid (R^2, 0.999). (R^2, 0.998). The Karl Fischer Moisture Analyzer was used to measure the water content. The Karl Fisher coulometer's measurement accuracy was tested using an HYDRANAL-water standard. The greatest standard deviations for water content analysis were less than 5%.

2.3 DESs preparation

The heating and mixing procedure described in [32], was used to prepare deep eutectic solvents (DESs). Tetrabutyl ammonium hydrogensulphate (TBAHS) and *p*-toluene sulfonic acid monohydrate (PTSAM) were mixed in a Schott bottle at a specific molar ratio of 1:2, heated to 80°C for 3 hours, and mixed using Teflon magnetic bars; the produced catalyst is henceforth referred to as N-DES. An in-depth catalyst characterization is performed elsewhere [33], and key properties are included in Table 2. The key property to observe is the increased H_0 acidity value compared to the previously developed catalyst where H_0 value was 0.42 [33].

Table 2. Important properties of novel ammonium-based catalyst, N-DES.

	Molar mass (g/mol)	Melting point	Water content (%)	Mass loss %	Mass Density	Dynamic viscosity	H_0*
N-DES	239.99	-43.18 °C	4.50	1.75 % (25-130 °C)	1.125 g/cm^3 (at 90 °C)	0.055 Pa-s (at 90 °C)	-2.91 (aqueous solution)

* H_0 represents the Hammett acidity value.

3 Results and discussion

3.1 Esterification with model reactants

At various temperatures (90 °C, 110 °C, 130 °C, and 150 °C) and catalyst concentrations (1, 5, and 10 wt.%), oleic acid was esterified with glycerol in the presence of the novel quaternary ammonium-based catalyst. The temperature and catalyst concentration ranges were established based on the previous study [28]. Figs 1(a) to 1(d) illustrate the FFA conversion vs Time for varying catalyst concentrations at different temperatures. Initially, the reaction rate and equilibrium conversion are observed to be catalyst dosage dependent, as shown most clearly in Fig. 1a, where different catalyst loading is used at 90°C. In Fig. 1a, with 1, 5, and 10 wt. % catalyst loading, the equilibrium conversion at 90 °C is 5%, 88% (no equilibrium) and 89%, at 60-minute mark, respectively. It may be implied here that, even with a higher reaction temperature and maximum catalyst concentration possible (within the scope), the reactions performed at 90 ℃ still could not reach maximum equilibrium conversion (94%), as observed consistently at other reaction temperatures. Furthermore, negligible conversion (<1%) was found at 90 ℃ in a non-catalyzed glycerolysis reaction extending over 5 hours of reaction time. These observations may imply that: 1) it is possible that within reaction time considered, equilibrium may not be reached even with increasing the maximum possible concentration for given homogenous catalyst; or 2) perhaps a more appealing logic: it is difficult to remove moisture at such low temperature to push reaction in desired direction. In Fig. 1(b), with 1, 5, and 10 wt. % catalyst loading, the equilibrium conversion at 110 °C is 25% (no equilibrium), 94%, and 94%, at 150, 120, and 120-minute mark, respectively. The effect of catalyst dosage at this temperature was observed with difference in the slopes of the conversion rate for 5% and 10% catalyst loading, even when the equilibrium is reached at similar times. In Fig. 1(c) at 130 °C, with5 and 10 wt. % catalyst loading, the equilibrium conversion at 130 °C is 94% and 94%, at 45 and 10-minute mark, respectively. However, equilibrium conversion is not achieved for 1 wt.% catalyst dosage (85% conversion) within considered reaction time. In Fig. 1(d), with 1, 5, and 10 wt. % catalyst loading, the maximum equilibrium conversion (94%) at 150 °C was observed, at 120, 10, and 5-minute mark, respectively. In Figs 1(c) and 1(d), it can be seen that an increase in the temperature results in a reduction in equilibrium conversion time.

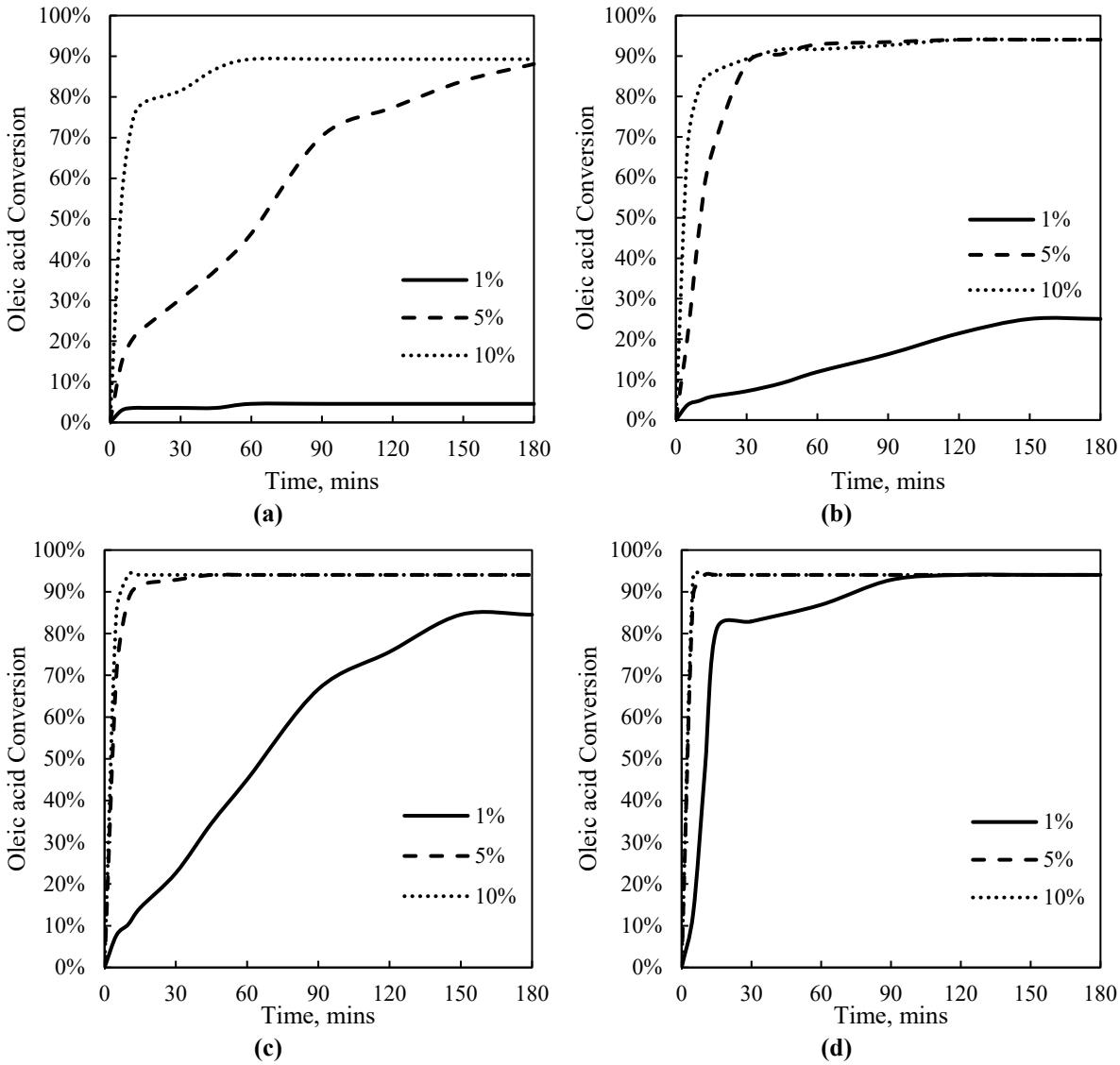


Fig. 1. Oleic acid conversion vs Time, for varying catalyst dosage with varying temperature; (a) 90 ℃, (b) 110 ℃, (c) 130 ℃, and (d) 150 ℃ (overlapping of 5% and 10% catalyst dosage curves).

3.1.1 Reaction kinetics

Reaction kinetics is required to measure reaction rates, characteristics that influence the rate of a chemical reaction, and to gain insight into reaction mechanisms. Understanding the kinetics of a reaction is essential for controlling and directing the intended reaction outcomes. As temperature and time were already optimised in section 3.1, the selected variable in the kinetics study is catalyst dosage, and the desired outcome is to maximise product yield.

Assuming a second-order rate equation for glycerolysis of oleic acid, the reaction rate equation, Eq. (1) can be written as below:

$$r = kC_{Gly}C_{OA} \quad (1)$$

However, when the reactant glycerol is introduced in excess, the equation can be assumed to be pseudo-first order with a reaction rate dependent on the limiting reactant oleic acid, as shown below in Eq. (2):

$$r = k' C_{OA} \tag{2}$$

where, k is the second order rate constant and k' is pseudo-first-order rate constant. C is for molar concentration, and subscripts *Gly* and *OA* stand for glycerol and oleic acid. Eq. (3) presents the mole balance equation for a batch reactor, where X_0 is the conversion, and N_{o0} is the initial moles of oleic acid and t is reaction time, V is the volume of the reactor,

$$\frac{\mathrm{d}X_0}{\mathrm{d}t} = \frac{-rV}{N_{O_0}} \tag{3}$$

By combining the above equations, Eq. (4) is obtained and by integrating this equation, Eq. (5) is achieved:

$$\frac{\mathrm{d}X_0}{\mathrm{d}t} = k'(1 - x_0) \tag{4}$$

$$k' = \frac{-ln(1-X_0)}{t} \tag{5}$$

By plotting ln(1-X_0) against time t, k' was obtained and then using the Eq. (6), the activation energy (E_A) for different catalyst dosing can be determined.

$$\ln\left(k`\right) = -\frac{E_A}{R}\left(\frac{1}{T}\right) + \ln(A) \tag{6}$$

where, A is the pre-exponential factor, and R is the universal gas constant.

Fig. 2 shows the plot of ln*(k')* versus 1/*T*. The gradient of each slope was multiplied by the universal gas constant (R) to calculate the activation energy at the different catalyst loading, shown in Fig. 3; the errors in activation energy calculations are entirely fitting based. E_A for 1% catalyst loading was found to be approximately 64.52 (± 9.56) KJ/mol, with increase in the catalyst concentration to 5%, the E_A drops slightly to approximately 55.72 (± 7.49) KJ/mol. However, a significant drop in activation energy was achieved with increasing catalyst concentration to 10%, where the lowest value for E_A i.e., approximately 16.18 (± 2.23) KJ/mol was achieved. At 10% catalyst loading, the drop in E_A allows the reaction to reach the equilibrium conversion in a lesser reaction time. The increased concentration of the N-DES (10%) the reaction facilitates completion under more mild conditions, with a shortened reaction time.

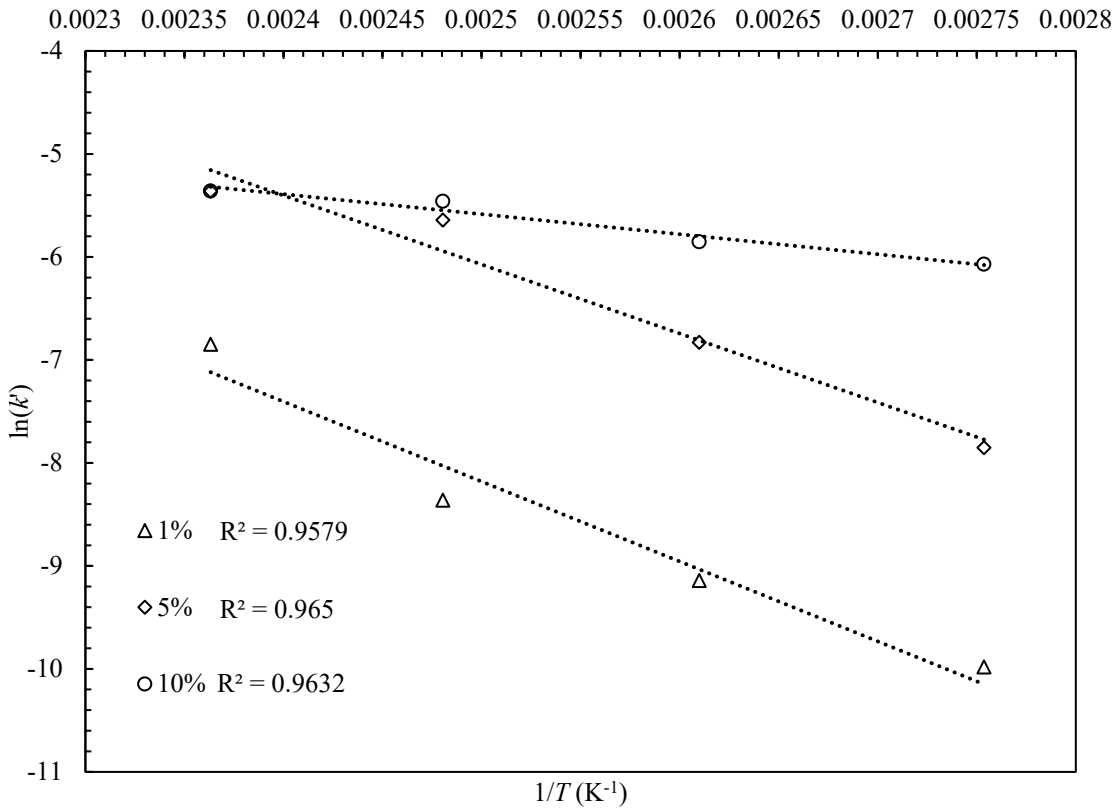


Fig. 2. Effect of catalyst loading on the activation energy for N-DES Catalyst.

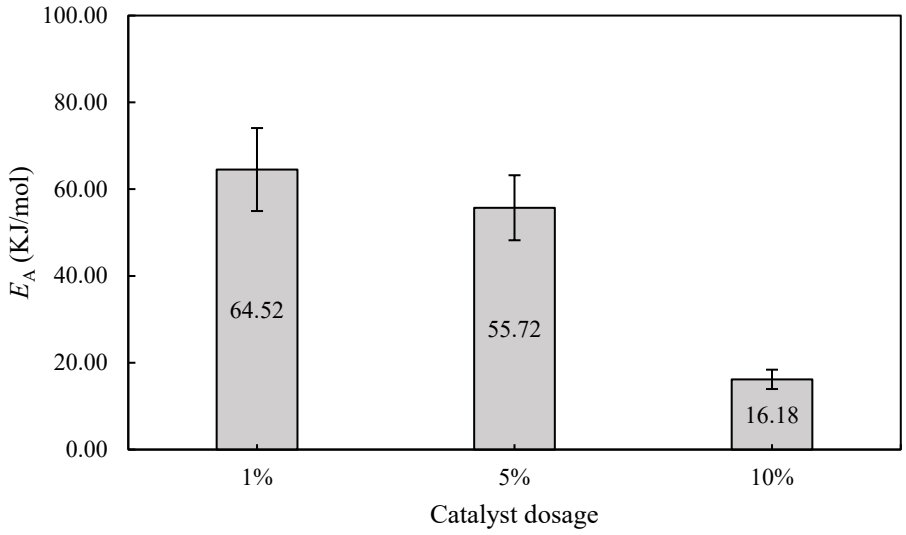


Fig. 3. Effect of catalyst loading on the activation energy, E_A.

3.1.2 Optimum conditions

As observed in Fig. 3, the least activation energy was obtained at 10% catalyst dosage. For further investigation into optimum conditions, 10% catalyst loading was selected. It was observed that for the 10-minute mark, conversion reaches equilibrium for 130℃; thus, 130℃

and 10% catalyst loading were considered optimum reaction conditions, as shown in Fig. 4. These optimum conditions suggest that considerable improvement in reaction time and the temperature was attained with the novel catalyst we have developed over the benchmark catalyst where 95% equilibrium conversion in 30 minutes of reaction time at 150 ℃ was reported [28].

Moving on, an improvement in the product selectivity/yield in ascending order of mono-, di- and lowest amount of triolein is desired, as this lowers the energy input required in transesterification reaction to produce fatty acid methyl esters (FAMEs) simply known as crude biodiesel [34]. At the optimum conditions, the change in the molar composition of the fatty phase during the reaction is shown in Fig. 4. This plot implies that a parallel product formation is occurring. During the first five minutes of the reaction majority of monoolein was produced with some diolein and triolein produced in parallel. While as the reaction continued, the quantities of each glycerides rose until equilibrium was reached at the 10-minute mark. The product yield determined at the end of the reaction was approximately, 65% for monoolein, 18.3% for diolein, and 10.7% for triolein. As more monoolein was produced here, the selectivity was also improved from the benchmark study used during this investigation [28], where mono- (27%), di- (58%) and tri-olein (9%) content was reported.

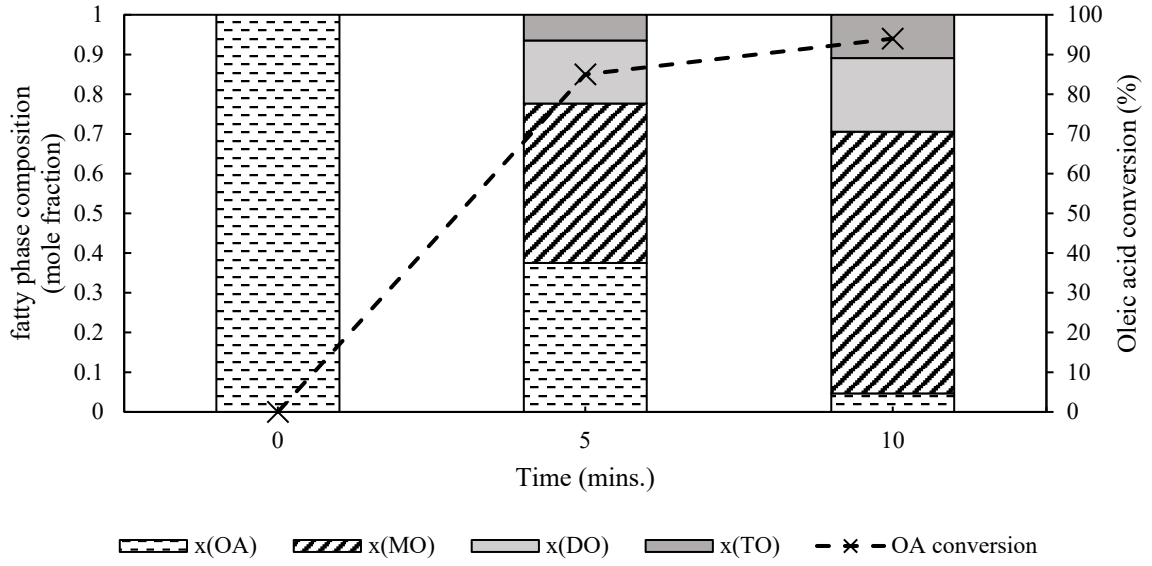


Fig. 4. Oleic acid conversion (solid dashed lines scaled to right y-axis), and change in the molar composition (stacked columns scaled to left y-axis) of fatty phase in the glycerolysis reaction using novel synthesized catalysts at optimum conditions with respect to Time: 130°C and 10 wt.% catalyst loading.

A plausible reaction mechanism in the presence of N-DES catalyst considering only product formation for monoolein is discussed as following: At the beginning of the reaction, the catalyst having polar and non-polar ends, creates a liquid-liquid interface, where glycerol was available for reaction with fatty acid moiety. Then the reaction proceeds with the protonation of the carbonyl group of oleic acid by the catalyst to make it easier for glycerol's nucleophilic attack on the carbonyl group. After the rearrangement of tetra-intermediate formed, monoolein and water were produced. For diolein and triolein formation, only the reactant molecule changes from oleic acid to monoolein or diolein, as per product glyceride

3.1.3 Deteriorating effects of water

The equilibrium conversion was found to be 94% at optimum conditions, indicating 6% FFA was still unreacted. A similar equilibrium (95%) at optimum conditions was reported in the benchmark study [28], however, the cause of this incomplete conversion was not investigated in depth. During the present study, it was hypothesised that the presence of water produced during the reaction limits the complete conversion. To investigate this, the reaction was carried out at optimum conditions with aggressive nitrogen (N_2) purging (1000 mL/min) for 3 hours with an aim of sweeping all the water produced out of the reaction. Instead of aiming to produce a nitrogen blanket (N_2 - 120 mL/min) during the reaction as was the case until now, the N_2 was purged through the reaction volume. This was done, as during the reaction, it was found that even with aggressive N_2 purging if the N_2 was not passed through the reaction volume, i.e. the homogenised reaction media, there was little to no effect on water removal. Samples were drawn throughout the reaction and the glycerol phase was tested for water content. Fig. 5 shows the plots of oleic acid conversion (Left y-axis) and water content in the glycerol phase (Right y-axis) during the course of the reaction. The water content during regular N_2 purging was constant at 3.93% around the 15-minute mark, while during aggressive N_2 purging, a much lower water content of 0.39% was attained around the 120-minute mark. It was clearly observed as the water gets removed from the reaction, the equilibrium conversion changes from 94% to almost complete conversion (98.8 %) at the 60-minute mark. This experiment, with changing N_2 purging rate, proved the initial conjecture to be true i.e., the water, a by-product of the reaction, impeded the extent of equilibrium conversion.

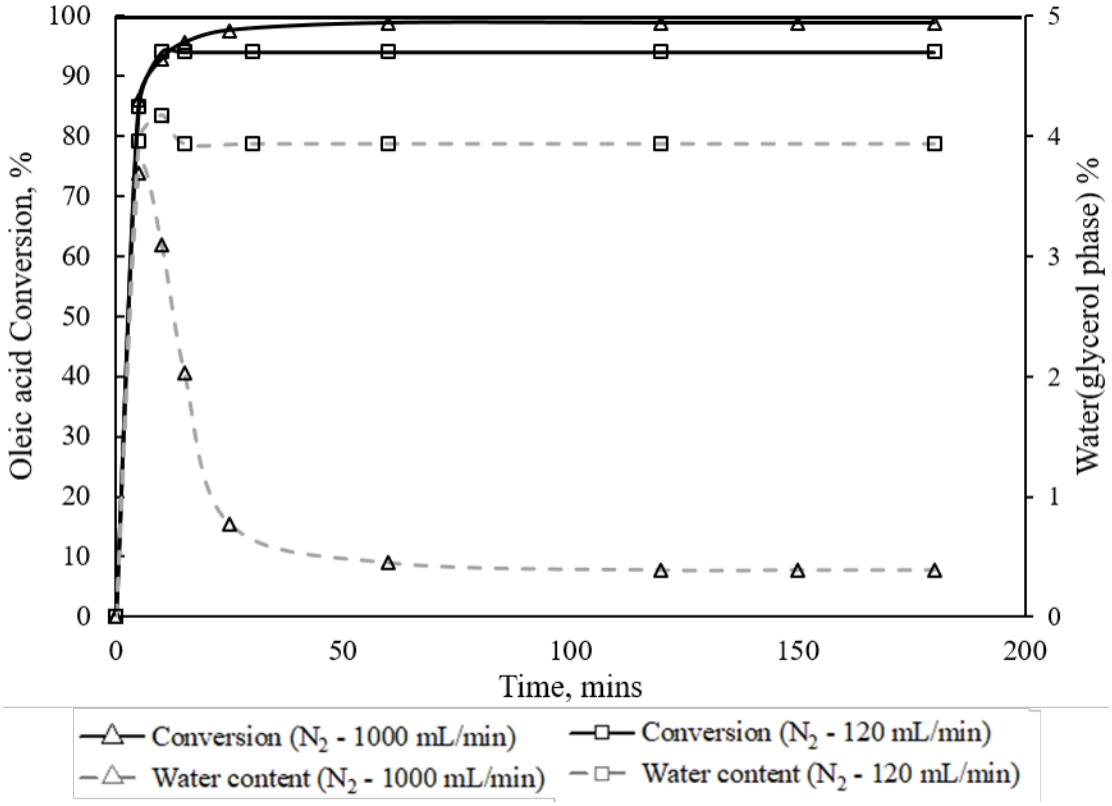
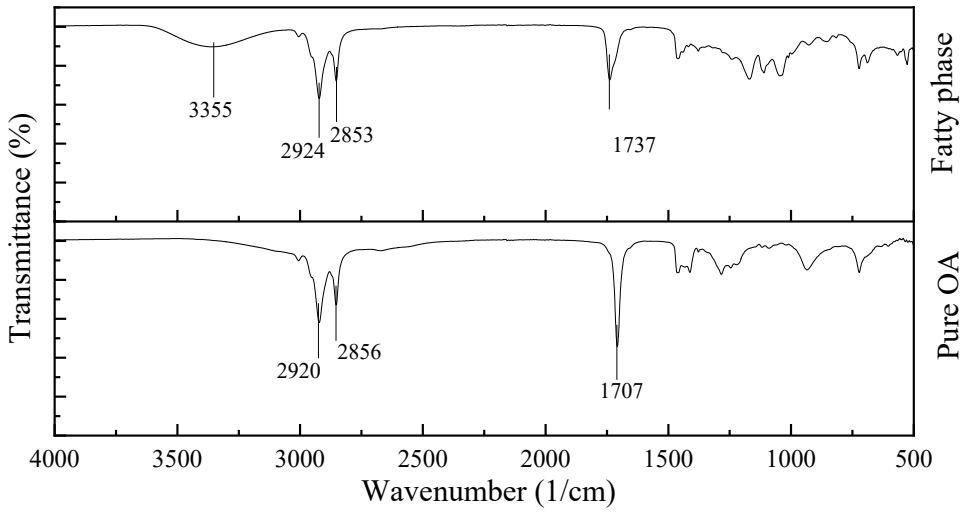


Fig. 5. Effect of nitrogen purging rate on oleic acid equilibrium conversion. Solid lines are scaled on the left y-axis and dashed lines are scaled on the right y-axis.

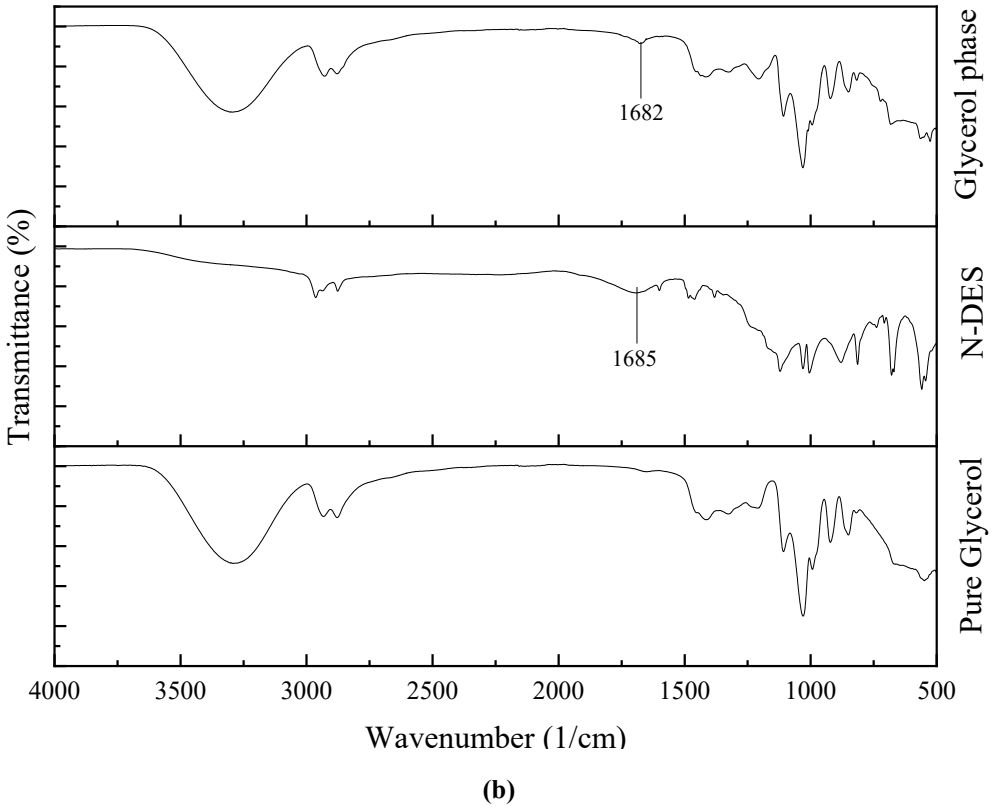
3.1.4 Confirmation of glyceride formation and catalyst location

FT-IR ATR technique was used to confirm the formation of glycerol esters of oleic acid during the reaction. This technique also showed potential in determining the presence of the catalyst in the glycerol-rich phase. As the DESs tested for catalytic capacity in this study are hydrophilic, it was hypothesised that the glycerol phase will contain all of the catalyst as a homogeneous mixture of glycerol, by-product water, and the catalyst. At the end of the reaction, both visually discernible layers were investigated using FT-IR-ATR (fatty phase and glycerol phase). Fig. 6(a) shows FT-IR spectrums of pure OA and fatty phase after reaction at optimum conditions. For pure OA, a carboxylic C=O stretching band was observed at 1707 cm^{-1}. Two intensive peaks at 2924 cm-1 and 2853 cm^{-1} are considered to be the carbon chains of OA. The absorption band of an ester C=O (1750-1735 cm^{-1}) is generally upfield than C=O (1720-1706 cm^{-1}) of a carboxylic acid [35]. As seen in Fig. 6(a), the C=O band in the fatty phase has shifted to 1737 cm^{-1}, indicating the formation of an ester bond. The appearance of a wide band (3355 cm^{-1}) in the fatty phase demonstrates the intermolecular H-bonding of O-H group from mono- and di-olein.

Moving on, the absence of C=O stretching bond in the pure glycerol is a critical evidence in determining whether esters solubilise in the glycerol phase or not. Fig. 6(b) shows the FT-IR spectrums of pure glycerol, N-DES and glycerol phase after the reaction completion. Evidently, no C=O stretching bond was observed in FT-IR spectrums of either pure glycerol or glycerol phase. Thus, it was confirmed that esters of oleic acid are formed as products and stay in the fatty phase. Furthermore, as catalyst was only present in lesser quantity (10 wt. %) than reactants, it was expected that absorption bands from glycerol or esters would be much stronger than of the N-DES. Additionally, the catalyst was composed of 1:2 molar ratio of TBAHS and PTSAM, so absorption bands of PTSAM are expected to be stronger. In Fig. 6(b), the FT-IR spectra of N-DES shows that absorptions bands are mainly in the 500-1700 cm^{-1} region. The wide shoulder region marked at 1685 cm^{-1} in the N-DES spectra arises from the methyl and sulfonic group substitutions at the para level on the benzene ring in PTSAM [36]. The appearance of a weak and slightly broadened peak at 1682 cm^{-1} in the glycerol phase which was not present in pure glycerol, may indicate the presence of the catalyst in the only glycerol layer. Hence, it was concluded that the catalyst was present in the glycerol phase after the reaction completion. As such, the glycerol phase itself was recycled and reused to investigate the catalyst reusability studies.



(a)



(b)

Fig. 6. (a) FT-IR spectra of pure oleic acid and fatty phase after the glycerolysis reaction using N-DES catalyst; (b) FT-IR spectra of pure glycerol, N-DES and glycerol phase after the glycerolysis reaction using N-DES catalyst.

3.1.5 Catalyst recyclability

Catalyst reusability is crucial for a catalyzed chemical reaction's economic and long-term viability. In the chemical industry, quick and easy catalyst reusability processes are frequently the most anticipated outcomes. While heterogeneous catalysts are commonly perceived to be quite reusable, homogeneous catalysts are frequently thought to be not particularly reusable, as the related separation/purification stages being extremely energy intensive, usually. As the catalyst was observed to be present in the glycerol-rich phase after the reaction completion, the entire bottom layer was recycled after gravity separation to assess the reusability of the catalyst. Fresh glycerol was added to make up for: 1) the glycerol used in the previous reaction and; 2) the glycerol lost during transfers. It was ensured that losses due to the highly viscous nature of the glycerol phase were minimal during the transfer of feed from the reaction vessel to the separatory funnel to the reaction vessel again. As a result, these losses could not be attributed to a decrease in catalyst concentration and ultimately limit the conversion of recycled runs. Understanding the effect of water on equilibrium conversion, it was decided to investigate further the effect of water in the lower phase on catalyst reusability. Fig. 7, shows the catalyst

reusability over five cycles with or without water removal from glycerol phase. It was clear to observe the significant effect of water present in the glycerol layer and its removal. Without water removal, the conversion drops to approximately 40.7% at the end of 5th cycle, whereas with consistent water removal, the catalyst manages to be reusable with approximately 62.5% conversion at the end of 5th cycle. Similar phenomenon has been mentioned in literature, where the catalyst performance dropped during recycling [22]. In contrast to reusability results in this investigation, no drop in conversion efficiency was reported for up to five recycles without any water removal step when a different hydrogen bond acceptor, allyltriphenyl phosphonium bromide was used [28]. A plausible reason behind this might be the increased acidity of N-DES used here [33] which might have influenced some side reactions with glycerol during the oven evaporation stage. DESs degradation might also have contributed towards the drop in catalyst conversion efficiency. This degradation can occur via internal esterification reactions taking place over time between the acid part in (HBD) and the -OH (HBA) in the DESs [22]. Another important consideration here would be incomplete water removal after oven evaporation, as 100 °C, is not sufficient temperature. The other strategies would be industrially practiced rotary steaming, vacuum distillation or using an adsorbent. However, fate of catalyst would remain a worry, requiring further investigation.

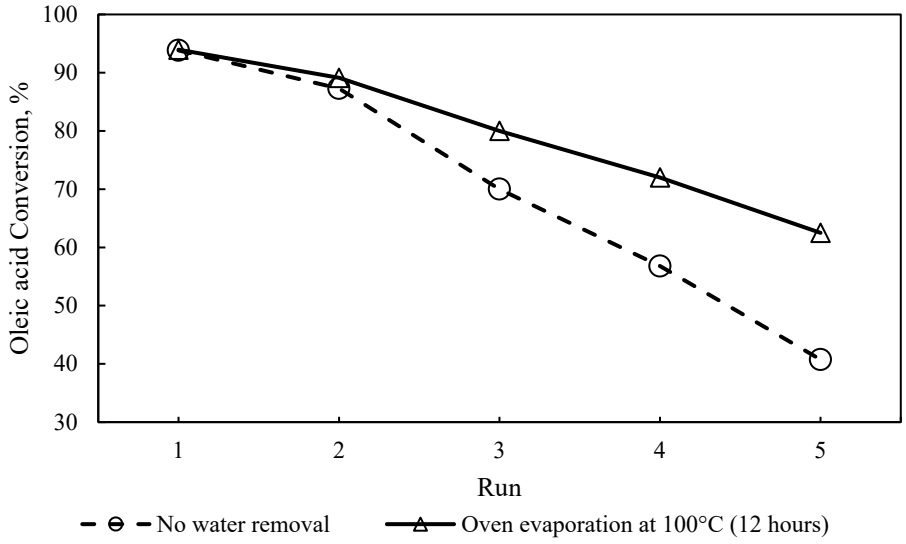


Fig. 7. Effect of water in recycled glycerol phase on reusability of the catalyst.

3.2 Effect of different feedstock at optimized conditions

To test the catalyst performance with real feedstock, both reactants were changed selectively initially. Oleic acid was replaced with Palm fatty acid distillate (PFAD) and brown grease

(BG), reacted with pure glycerol. While for crude glycerol, grades CG1 and CG2 replaced pure glycerol and reacted with pure oleic acid. Table 1 shows the feedstock composition and Fig. 8 shows the FFA conversion vs reaction time plot for the four different feedstock investigated. For PFAD and BG reacted with pure glycerol, approximately similar equilibrium conversion of 93.3%, as in the case of pure oleic acid, was achieved. One plausible reason behind this feedstock flexibility might be the dominant presence of oleic acid in the composition of majority of non-edible high FFAs feedstock [8]. This shows that catalyst was capable of handling different feedstock of varying origins and the developed process can handle feedstock such as waste cooking oils (FFAs rich) from Food and Hospitality industry.

In the case of crude glycerol, the 15-minute conversions of CG1 and CG2 with pure oleic acid are approximately 44.7% and 88.4%, respectively. While water, the primary impurity in CG2 (Table 1), has already been shown to degrade FFA conversion, the decline in conversion was comprehensible. Side reactions with MONG and deactivation by ash, among many additional pathways in which the catalyst may be hampered in interacting with FFA and glycerol, are possible reasons for reduced FFAs conversion in the case of CG1. It was justified to conclude that present catalyst shows flexibility towards varying high FFAs feedstock but good quality glycerol was necessary.

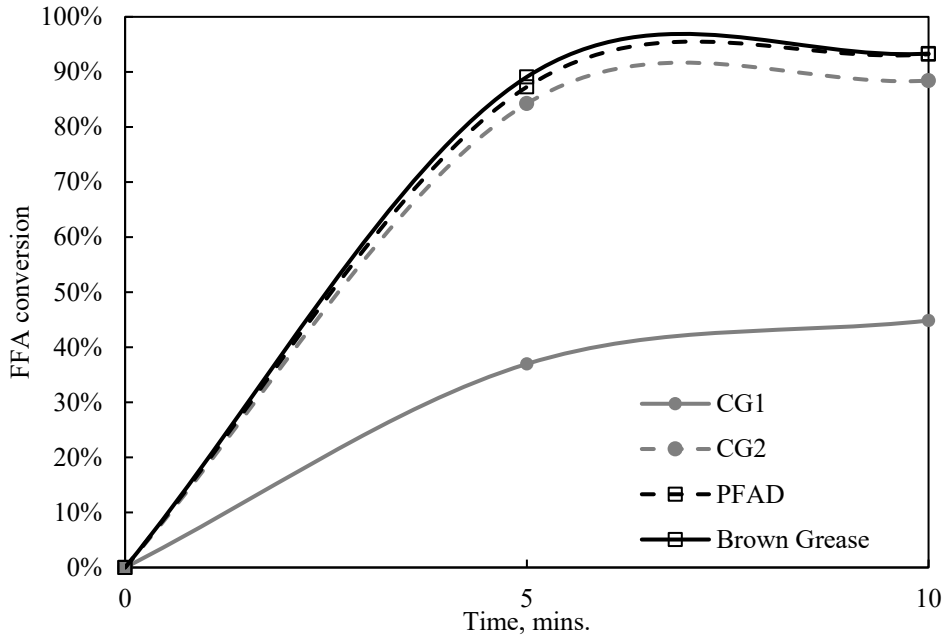


Fig. 8. Performance of N-DES in glycerolysis using different feedstock.

Moving on, it is imperative to consider the cost associated with synthesizing the benchmark catalyst [28] and the catalyst (N-DES) developed for the lab-scale glycerolysis pre-treatment.

In addition to N-DES constituting 1 mole lesser of PTSAM than benchmark DESs, the effective price of HBA is also lower for N-DES. For synthesizing 100 grams of the benchmark catalyst and N-DES, the latter was approximately 13% cheaper. The purchase prices were quoted from the chemical supplier, Sigma-Aldrich.

4 Conclusion

A novel DES based on quaternary ammonium salt and PTSAM was tested in the glycerolysis of oleic acid. The optimum conditions of 130 ℃, 10 minutes, 10 wt.% catalyst loading, 6:1 (glycerol to oleic acid molar ratio), 600 rpm stirring, and 80-120 mL N_2 purging, gave approximately 94% equilibrium conversion. The product yields achieved for monoolein, diolein and triolein, were 65%, 18.3% and 10.7% respectively. The reactions to monoolein, diolein and triolein were found to happen in parallel. The acidic anionic complex part of catalyst accelerated the nucleophilic substitution reaction, where in its absence glycerol was found to be a weak nucleophile. The bulkier cationic part of the catalyst increased the mass transfer between the two nearly immiscible reactants, creating a liquid-liquid interface in a biphasic system. The application of catalyst at optimum loading of 10 wt.% provides a significant drop in activation energy, providing reaction completion at lower reaction temperature and lesser reaction time. After the reaction was completed and cooled down, FT-IR investigations revealed that the catalyst being polar was present in the bottom layer (glycerol phase). Water was found to be detrimental to equilibrium conversion and catalyst reusability. Removing water pushed near complete conversion was achieved in 60 minutes. In a catalyst reusability investigation, when oven evaporation was applied, the catalyst reusability was increased, approximately 62.5% conversion in the 5^{th} cycle, while in the absence of the oven evaporation step, the 5^{th} cycle conversion was approximately 40.7%. Industry-grade feedstock showed similar conversion as that of pure oleic acid. For crude glycerol, water deteriorated the conversion; CG1 contained other impurities which further deteriorated the conversion. Water being a by-product in the esterification of FFAs, and a likely substantial impurity in industry-grade feedstock, its removal is required to achieve good FFAs conversion. This necessitates further research into the effective removal of water during the process to mitigate its negative consequences.

Declaration of Competing Interest

The authors declare that they have no known competing financial interests or personal relationships that could have appeared to influence the work reported in this paper.

Acknowledgements

We acknowledge the New Zealand Government through the Ministry of Foreign Affairs and Trade (MFAT) for providing New Zealand Development Scholarships. We are grateful towards BAKELS Edible Oils NZ Ltd. for supplying PFAD samples, SABREnergy Australia for providing brown grease samples, and Green Fuels NZ Limited for supplying Crude glycerol samples, essential for this research. We acknowledge Dr Matthew Sidford, Technical Manager, Chemical and Materials Engineering department, The University of Auckland, for his support with analytical measurements throughout this study. We also acknowledge Raymond Hoffmann (Senior Technician), Chemical and Materials Engineering department, The University of Auckland, for his support with fabrication of the reaction vessel and associated auxiliaries.

References

1. Rashid, U., et al., Production of sunflower oil methyl esters by optimized alkali-catalyzed methanolysis. Biomass and Bioenergy, 2008. **32**(12): p. 1202-1205.
2. Ong, H.C., et al., Life cycle cost and sensitivity analysis of palm biodiesel production. Fuel, 2012. **98**: p. 131-139.
3. Guan, G., et al., Transesterification of vegetable oil to biodiesel fuel using acid catalysts in the presence of dimethyl ether. Fuel, 2009. **88**(1): p. 81-86.
4. Spinelli, D., et al., Environmental and life cycle analysis of a biodiesel production line from sunflower in the Province of Siena (Italy). Energy Policy, 2013. **59**: p. 492-506.
5. Habibullah, M., et al., Biodiesel production and performance evaluation of coconut, palm and their combined blend with diesel in a single-cylinder diesel engine. Energy Conversion and Management, 2014. **87**: p. 250-257.
6. Karmakar, B. and G. Halder, Progress and future of biodiesel synthesis: Advancements in oil extraction and conversion technologies. Energy Conversion and Management, 2019. **182**: p. 307-339.
7. Ribeiro, A., Castro, F. and Carvalho, Joana, Influence of free fatty acid content in biodiesel production on non-edible oils, in WASTES: Solutions, Treatments and Opportunities 1St International Conference. 2011, Centre for Waste Valorization.
8. Shahidi, F., Bailey's Industrial Oil and Fat Products, 6th Edition, 2005, John Wiley and Sons. p. 648-1292.
9. Manaf, I.S.A., et al., A review for key challenges of the development of biodiesel industry. Energy Conversion and Management, 2019. **185**: p. 508-517.
10. Naylor, R.L. and M.M. Higgins, The political economy of biodiesel in an era of low oil prices. Renewable and Sustainable Energy Reviews, 2017. **77**: p. 695-705.
11. Bentivoglio, D., et al., Asian Palm Oil Production and European Vegetable Oil Market: What Can We Learn in Terms of Sustainability?, in Asian Nations and Multinationals: Overcoming the Limits to Growth, B. Andreosso-O'Callaghan, J. Jaussaud, and M.B. Zolin, Editors. 2018, Springer International Publishing: Cham. p. 83-99.
12. Ashraful, A.M., et al., Production and comparison of fuel properties, engine performance, and emission characteristics of biodiesel from various non-edible vegetable oils: A review. Energy Conversion and Management, 2014. **80**: p. 202-228.
13. Balat, M., Potential alternatives to edible oils for biodiesel production – A review of current work. Energy Conversion and Management, 2011. **52**(2): p. 1479-1492.

14. Fereidooni, L. and M. Mehrpooya, Experimental assessment of electrolysis method in production of biodiesel from waste cooking oil using zeolite/chitosan catalyst with a focus on waste biorefinery. Energy Conversion and Management, 2017. **147**: p. 145-154.
15. Fonseca, J.M., et al., Biodiesel from waste frying oils: Methods of production and purification. Energy Conversion and Management, 2019. **184**: p. 205-218.
16. Kinast, J.A., Production of Biodiesels from Multiple Feedstocks and Properties of Biodiesels and Biodiesel/Diesel Blends: Final Report; Report 1 in a Series of 6. 2003: United States.
17. Sahani, S., T. Roy, and Y.C. Sharma, Studies on fast and green biodiesel production from an indigenous nonedible Indian feedstock using single phase strontium titanate catalyst. Energy Conversion and Management, 2020. **203**: p. 112180.
18. Roslan, N.A., N. Abdullah, and S.Z. Abidin, The synthesis of sulphonated hypercrosslinked exchange resin for free fatty acid esterification. Comptes Rendus Chimie, 2019. **22**(11-12): p. 761-770.
19. Mehrpooya, M., B. Ghorbani, and H. Abedi, Biodiesel production integrated with glycerol steam reforming process, solid oxide fuel cell (SOFC) power plant. Energy Conversion and Management, 2020. **206**: p. 112467.
20. Sonntag, N.O.V., Glycerolysis of Fats Status, Review and and Methyl Esters-- Critique. Journal of the American Oil Chemists' Society, 1982.
21. Mamtani, K., K. Shahbaz, and M.M. Farid, Glycerolysis of free fatty acids: A review. Renewable and Sustainable Energy Reviews, 2021. **137**: p. 110501.
22. Mamtani, K., K. Shahbaz, and M.M. Farid, Deep eutectic solvents – Versatile chemicals in biodiesel production. Fuel, 2021. **295**: p. 120604.
23. Smith, E.L., A.P. Abbott, and K.S. Ryder, Deep eutectic solvents (DESs) and their applications. Chem Rev, 2014. **114**(21): p. 11060-82.
24. Qin, H., et al., Bifunctional imidazole-PTSA deep eutectic solvent for synthesizing long-chain ester IBIBE in reactive extraction. AIChE Journal, 2018. Doi: 10.1002/aic.16472
25. Zhou, Y., et al., Reactive extraction for synthesizing long chain ester butyl hexanoate intensified by deep eutectic solvent. Chinese Journal of Chemical Engineering, 2021. 36: p. 120-127.

26. Wang, R., et al., Toward reactive extraction processes for synthesizing long-chain esters: A general approach by tuning bifunctional deep eutectic solvent. Chemical Engineering Journal, 2022. 445: p. 136664.
27. Lyazzat Zhanenova , S.B., Mohammed M. Farid, Improving the economics of biodiesel production through esterification of free fatty acid with waste glycerol., in Engineering Our Future: Are We up to the Challenge? 2009, Engineers Australia: Barton, ACT.
28. Williamson, S.T., et al., Application of deep eutectic solvents as catalysts for the esterification of oleic acid with glycerol. Renewable Energy, 2017. **114**: p. 480-488.
29. Zhang, T., K. Shahbaz, and M.M. Farid, Glycerolysis of free fatty acid in vegetable oil deodorizer distillate catalyzed by phosphonium-based deep eutectic solvent. Renewable Energy, 2020. **160**: p. 363-373.
30. Gausas, L., et al., Catalytic hydrogenation of polyurethanes to base chemicals: from model systems to commercial and end-of-life polyurethane materials. JACS Au, 2021. **1**(4): p. 517-524.
31. Lubrizol Advanced Materials, Inc., Test Procedure, TP-TM-001C: Determination of Acid Value and Free Fatty Acid. 2009, The Lubrizol Corporation.
32. Marcus, Y. (2019). Deep Eutectic Solvents, Springer Nature Switzerland AG. p. 21.
33. Mamtani, K., et al., Investigations into the properties of acidic deep eutectic solvents based on p-toluenesulfonic acid. Unpublished results (2023), The University of Auckland.
34. Munack, A., Books: Biodiesel – A comprehensive handbook. Martin Mittelbach, Claudia Remschmidt (Ed.). Biotechnology Journal, 2006. **1**(1): p. 102-102.
35. Bellamy, L.J., Carbonyl Frequencies. In: The Infrared Spectra of Complex Molecules. 2012: Springer, Dordrecht. p. 128-194. https://doi.org/10.1007/978-94-011-6520-4_5.
36. Lin-Vien, D., et al., CHAPTER 17 - Aromatic and Heteroaromatic Rings, in The Handbook of Infrared and Raman Characteristic Frequencies of Organic Molecules, D. Lin-Vien, et al., Editors. 1991, Academic Press: San Diego. p. 277-306.

Table of contents (TOC) graphic

